Groundwater

Methods Note/

# A Physically Based Approach for Estimating Hydraulic Conductivity from HPT Pressure and Flowrate

by Robert C. Borden[1,2], Ki Young Cha[3], and Gaisheng Liu[4]

## Abstract

The hydraulic profiling tool (HPT) is widely used to generate profiles of relative permeability vs. depth. In this work, prior numerical modeling results are used to develop a relationship between probe advance rate $V$ (cm/s), probe diameter $D$ (cm), water injection rate $Q$ (mL/min), corrected pressure $P_c$ (psi), and hydraulic conductivity $K$ (feet/d)

$$K = E(0.1235\ VD^2 + 0.119Q){P_c}^{-1.017}$$

where $E$ is an empirically derived hydraulic efficiency factor. The relationship is validated by 23 HPT profiles that, after averaging $K$ vertically, were similar to slug test results in adjoining monitoring wells. The best fit value of $E$ for these profiles was 2.02. This equation provides a physically based approach for generating hydraulic conductivity profiles with HPT tooling.

## Introduction

Over the past two decades, a series of direct push (DP)-based field approaches (Dietrich and Leven 2009; McCall and Christy 2010; Liu et al. 2012; Maliva 2016) have been developed to characterize small-scale spatial variations in hydraulic conductivity ($K$) that control groundwater flow and contaminant transport in heterogeneous aquifers. One of the most effective approaches for directly estimating $K$ is direct push injection logging (DPIL) where water is injected through the probe at flowrate ($Q$) while monitoring changes in pressure. Figure 1 shows the hydraulic profiling tool (HPT) manufactured by Geoprobe Systems, Inc. (Salinas, Kansas) for DPIL logging. As the HPT probe is advanced through saturated formation material, water is injected through a port on the side of the probe while simultaneously monitoring injection rate at the surface and pressure closely behind the injection screen. The measured pressure ($P_m$) is the sum of hydrostatic pressure ($P_h$), atmospheric pressure ($P_a$), pressure generated by water injection ($P_i$), and pressure generated by displacement of aquifer material as the probe is advanced through the aquifer ($P_p$). Formation bulk electrical conductivity (EC) is measured near the bottom of probe to provide additional information on subsurface conditions (Schulmeister et al. 2003). HPT profiling has been established as an international standard practice by American Society for Testing and Materials (ASTM 2016) under ASTM designation D8037.

[1]North Carolina State University, Campus Box 7908, Raleigh, NC, 27695, rcborden@ncsu.edu

[2]Corresponding author: Emeritus Professor, Department of Civil, Construction and Environmental Engineering, North Carolina State University, Mailing Address and phone during COVID: 5017 Theys Rd, Raleigh NC 27606; 919-349-8473, rcborden@ncsu.edu

[3]Draper Aden Associates, 114 Edinburgh S Dr #200, Cary, NC, 27511

[4]Kansas Geological Survey, University of Kansas, 1930 Constant Ave, Lawrence, KS, 66047

*Article impact statement*: A simple, physically based equation is developed and field tested for estimating hydraulic conductivity from standard HPT data.

Received April 2020, accepted August 2020.

doi: 10.1111/gwat.13039

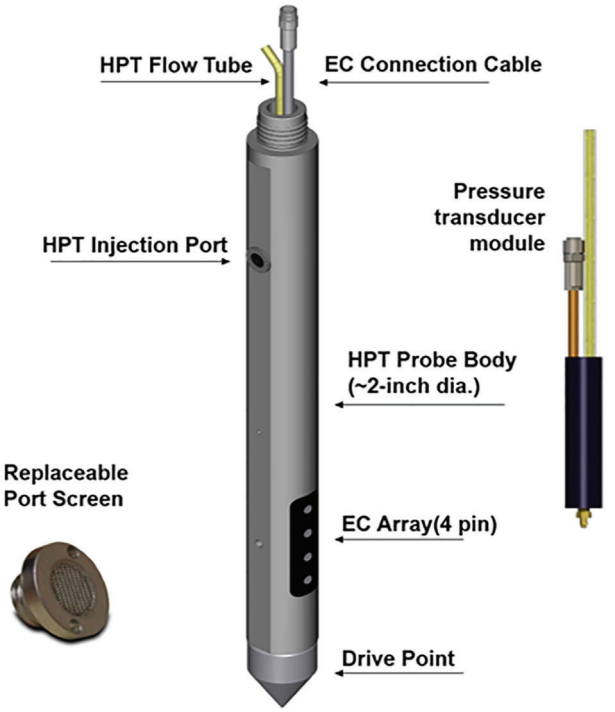


**Figure 1. Schematic of hydraulic profiling tool (HPT). During HPT profiling, water is injected through the flow tube and out of the screened port, and pressure is measured inside the connection rod right above the injection port (McCall et al. 2017).**

A variety of approaches have been used to relate water injection rate and pressure data acquired during HPT profiling to spatial variations in permeability. Cho et al. (2004) proposed using the ratio of water injection rate to pressure ($Q/P$) as an index of $K$. Dietrich et al. (2008), Liu et al. (2009), and Lessoff et al. (2010) generated profiles of $K$ vs. depth using site-specific empirical relationships between $Q/P$ and $K$. McCall and Christy (2010) developed an empirical relationship between $Q/P_c$ and $K$ measured in DP piezometers using pneumatic slug testing in an alluvial aquifer. Estimated $K$ is calculated

$$Est.K = 21.14 \ln\left(\frac{Q}{P_c}\right) - 41.71 \quad (1)$$

where $Q$ is the water injection rate through the HPT probe in mL/min and $P_c$ is the corrected pressure, $P_c = P_m - P_h - P_a$, and the pressure generated by probe advance ($P_p$) is assumed negligible. In Equation 1, $K$ is a linear function of the natural log of $Q/P_c$. However, based on numerical simulations by Liu et al. (2019), $K$ should be a largely linear function of $Q/P_c$ for moderately to highly permeable settings ($K > 10^{-6}$ m/s).

In this work, we present a physically based approach for estimating $K$ from $Q$ and $P_c$ data acquired during HPT profiling. This new approach is based on numerical simulations of the physical flow processes that take place during probe advance and water injection under different aquifer and HPT operation conditions (Liu et al. 2019). Average $K$ from HPT borings is then compared to $K$ estimates from slug tests in adjoining wells, and an empirical hydraulic efficiency factor ($E$) is developed to correct for changes in permeability near the probe.

## Background

Liu et al. (2019) completed a series of high-resolution numerical simulations to better understand the underlying physical processes controlling pore pressures during HPT profiling (Figure 2). The downward movement of the water injection screen during profiling was simulated as a sequence of vertical 1.5-cm intervals. Probe advance was approximated by injection of water around the tip at a rate equivalent to the volumetric rate of material displacement by the probe. The governing flow equation was numerically solved using COMSOL (www.comsol.com) due to its ability to accurately represent probe geometry. $Q$, $K$, specific storage ($S_s$), and probe advance speed ($V$) were systematically varied to investigate their impacts on HPT pressure distributions. Figure 2C shows an example distribution of simulated pore pressure increase due to probe advance and water injection. During the simulations, formation alteration, which likely happens in the field due to the materials being pushed aside by the probe, was not explicitly considered.

$P_c$ during HPT profiling may be increased if displaced soil forms a lower permeability zone around the HPT probe. When the HPT probe is advanced through saturated soil, high stresses near the probe tip cause local shear failure, and the plasticized soil is forced to the side, resulting in a disturbed zone surrounding the HPT probe. The disturbed zone typically has a diameter ($D_d$) that is 4 to 6 times the probe diameter ($D_P$), depending on the soil rigidity index (Burns and Mayne 1998). In normally consolidated soil, porosity ($n$) within the disturbed zone can decline as the excess pore pressure is released. Assuming the solid particles displaced by the advancing probe remain within the disturbed zone, the final porosity of soil within this zone will decline by 5% to 20%, depending on initial porosity and $D_d/D_P$. From the Kozeny-Carman equation (Chapuis and Aubertin 2003), $K$ is proportional to $n^3/(1-n)^2$, which implies $K$ may decrease by 20-50% within the disturbed zone. $K$ can decline further if sand and clay layers are mixed by shearing of the plasticized soil. Liu et al. (2019) examined the potential impacts of this disturbed zone on the apparent $K$ measured during HPT profiling by simulating a series of low-$K$ skins with varying thicknesses and reductions in $K$. However, the geotechnical processes leading to soil disturbance were not explicitly considered in the simulations.

### New Relationship for Estimating *K*

During HPT profiling, the pressure change observed at the water injection port is the sum of injection-induced pressure and the pressure change generated by probe advance. When the probe is rapidly advanced through lower $K$ aquifer material ($K < 10^{-6}$ m/s), high

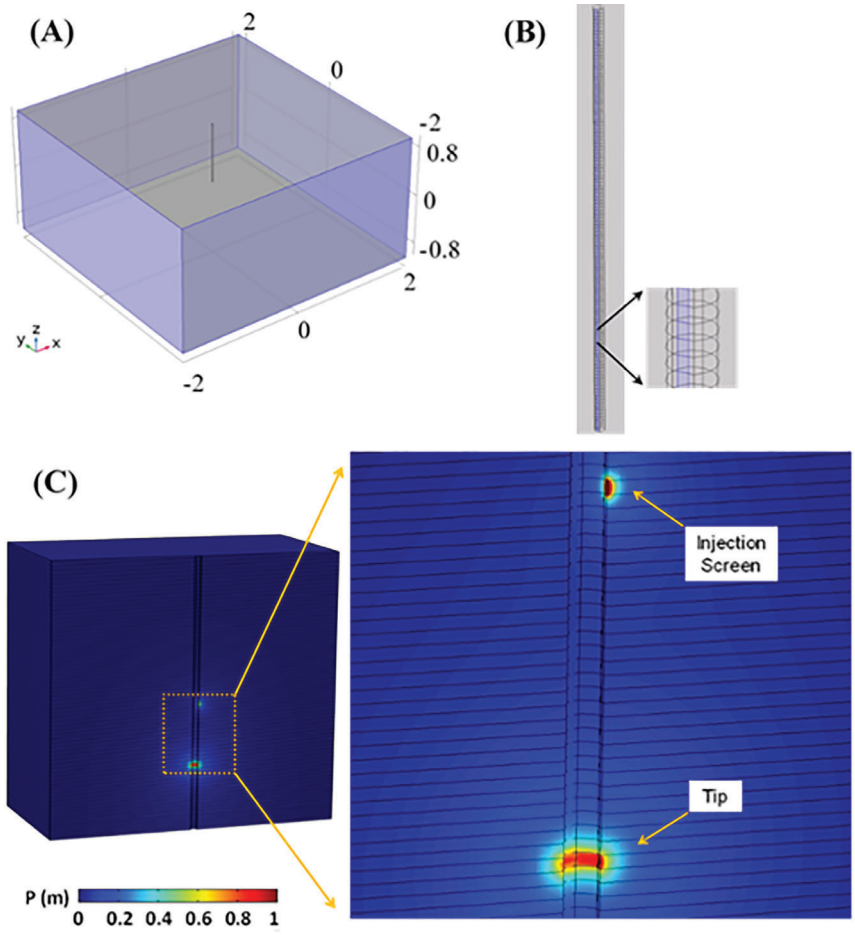


**Figure 2. Numerical model for pore pressure simulation during HPT profiling (after Liu et al. 2019): (A) a rectangular simulation domain of 4 by 4 by 1.8 m with the HPT probe at the center, (B) the moving injection screen simulated as a sequence of vertical 1.5-cm intervals during profiling, and (C) an example simulation of pressure increase due to probe advance and injection.**

pressures are generated at the probe tip, which produces a measurable change in pressure at the injection port. If the rate of probe advance is reduced, the pressure generated at the tip is decreased and there is more time for that pressure to dissipate before the injection port pressure sensor arrives at the tip location.

Liu et al. (2019) summarized the impacts of $Q$, $V$ and formation $K$ and $S_s$ on pressure at the injection port in curves relating $K/S_s$ to $Q/P_i/S_s$ and $Q_p/P_p/S_s$ (Figure 3). $Q$ is the flow rate of fluid injected through the HPT port. $Q_P$ is equivalent to the volume per unit time of groundwater displaced as the HPT probe is advanced through the formation material, with $Q_p = V*\pi D^2/4$, where $D$ is the HPT probe diameter.

Figure 3 shows that when $K/S_s$ is between $10^{-4}$ and $10^{-1}$ m$^2$/s, Log($Q_p/P_p/S_s$) and Log($Q/P_i/S_s$) are linear functions of Log($K/S_s$). In this range,

$$Q_p/P_p/S_s = \alpha_p (K/S_s)^{\beta p} \quad (2a)$$

$$Q/P_i/S_s = \alpha_i (K/S_s)^{\beta i} \quad (2b)$$

where $\alpha_p = 1.982$, $\beta_p = 0.953$, $\alpha_i = 0.0574$, and $\beta_i = 0.992$, based on the best fit lines matched to the simulation data (Figure 3). Rearranging and solving for the corrected pressure ($P_c$)

$$P_c = P_p + P_i = Q_p/(\alpha_p * S_s * (K/S_s)^{\beta p}) + Q/(\alpha_i * S_s * (K/S_s)^{\beta i}) \quad (3)$$

Figure 4 shows the relationship between $K$ and $P_c$ at different values of $S_s$, probe speed $V$, and $Q$, for varying $P_c$. For the considered ranges of parameter values, $S_s$ does not have a measurable impact on the $K$ vs. $P_c$ relationship. When $Q \geq 200$ mL/min, the impact of $V$ is also negligible. However, for $Q \leq 50$ mL/min, varying $V$ has a small but measurable impact. In contrast, varying $Q$ between 50 and 600 mL/min has a substantial impact on the $K$ vs. $P_c$ relationship. Most interestingly, the slope of $K$ vs. $P_c$ does not change substantially with $Q$.

$K$ cannot be solved for directly from Equation 3 for a set of given $P_c$, $S_s$, $Q$, and $Q_p$ values. However, $K$ can be found using an iterative procedure where $K$ values are continuously adjusted until the computed $P_c$ matches the measured value. Instead of this iterative procedure, we propose the use of Equation 4 to calculate $K$ from HPT data, using coefficients, $C_1$, $C_2$, and $C_3$, that

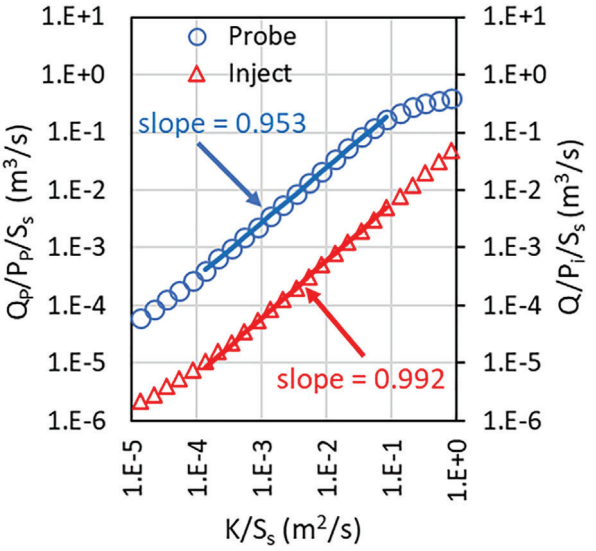


**Figure 3. Numerical simulation results from Liu et al. (2019) relating hydraulic diffusivity ($K/S_s$) to pressure generated by HPT probe advance ($P_p$, plotted to left axis) and fluid injection through the HPT probe ($P_i$, plotted to right axis). Note that the summation of $P_p$ and $P_i$ is the pressure change at the injection port that is measured during field HPT profiling.**

provide results equivalent to Equation 3. An empirically derived efficiency factor ($E$) is included to account for permeability loss in the disturbed zone surrounding the HPT probe.

$$K = E(C_1 V D^2 + C_2 Q)\, P_c^{C3} \tag{4}$$

$S_s$ was not included in Equation 4 since it did not have an appreciable impact on $K$. To find the best fit values of $C_1$, $C_2$, and $C_3$, Equation 3 is used to calculate $P_c$ for a range of $S_s$, $V$, $Q$, and $K$. $S_s$ was varied between 0.0003 and 0.003 $m^{-1}$, based on published $S_s$ values for unconsolidated aquifers (Freeze and Cherry 1979) and $S_s$ values measured in triaxial tests of aquifer material at Tulsa, OK (Borden et al. 2020). The numerical simulations used to generate Figure 3 assumed uniform isotropic soil, so $E = 1.0$ for these simulations. These data were sorted to eliminate any parameter combinations that would result in pressures outside the range that can be accurately measured with currently available equipment (0.7 to 70 m head or 1 to 100 psi) resulting in over 1700 unique combinations of $K$, $P_c$, $Q$, $V$, and $S_s$. The solver function in Microsoft Excel was used to search for values of $C_1$, $C_2$, and $C_3$ that minimized the normalized root mean squared error (NRMSE) between the reference $K$ and estimated values by Equation 4.

Best fit values of $C_1$, $C_2$, and $C_3$ are presented in Equation 5a for metric units ($K$ in m/s, $P$ in m of hydraulic head) and Equation 5b for English units ($K$ in feet/d, P in psi),

$$K(\text{m/s}) = E\left[4.061E-07\, V(\text{cm/s})\, D^2(\text{cm}) + 4.262E-07\, Q(\text{mL/min})\right] / P(\text{m})^{1.017} \tag{5a}$$

$$K(\text{feet/d}) = E[0.1235\, V(\text{cm/s})\, D^2(\text{cm}) + 0.119\, Q(\text{mL/min})] / P(\text{psi})^{1.017} \tag{5b}$$

Figure 5 shows a comparison between the reference $K$ in Equation 3 and estimated $K$ using Equation 5. Overall, Equation 5 provides an excellent match with the reference $K$ values. The NRMSE of estimated $K$ is less than 2%, which is considered excellent given that $K$ varies by three orders of magnitude.

### Field Evaluation of *K* Estimation Relationships

The new $K$ estimation approach is evaluated by comparing HPT results to slug test results from adjoining monitor wells, and to estimate an average hydraulic efficiency factor, $E$, to account for permeability reduction of aquifer material within the disturbed zone during HPT probe advance.

Slug tests are commonly applied in situ methods for estimating aquifer $K$. In this work, slug test results are interpreted using the Bouwer and Rice (1976) method. Numerical simulations of transient flow by Brown et al. (1995) show the Bower and Rice method can provide good estimates of $K$ in homogeneous formations, with errors of around 20% when the well screen is fully submerged. However, this method may underpredict $K$ due to when a lower $K$ skin is present (Zlotnik et al. 2010; Butler Jr. 2019). In heterogeneous formations, slug tests provide reasonable estimates of transmissivity over the screened interval (Beckie and Harvey 2002). While slug tests have weaknesses, most practitioners have a relatively good understanding of the strengths and limitations of this approach, and so a comparison with slug test measurements provdes a useful means to assess the reliability of HPT $K$ estimates.

Slug tests were conducted in 2-inch polyvinyl chloride monitor wells installed by hollow stem auger with a sand pack. The slug test was conducted by instantaneously adding or removing a weighted slug and measuring head response with a pressure sensor connected to a data logger. No corrections were made to account for vertical variations in $K$ over the screened interval. At least two slug-in and slug-out tests were conducted on each well. When the water table intersected the well screen, only the slug-out test results were used for analysis. The arithmetic mean slug test $K$ ($K_{slug}$) is computed and compared to the HPT results.

HPT Profiles of $K$ vs. depth were performed at 23 locations within 3 feet of an existing slug test well at four sites: Jacksonville, Selma, Greenville, and Tulsa. At each location, the 1.75-inch HPT Probe (Geoprobe 2015) with Wenner array was advanced while $Q$ was held

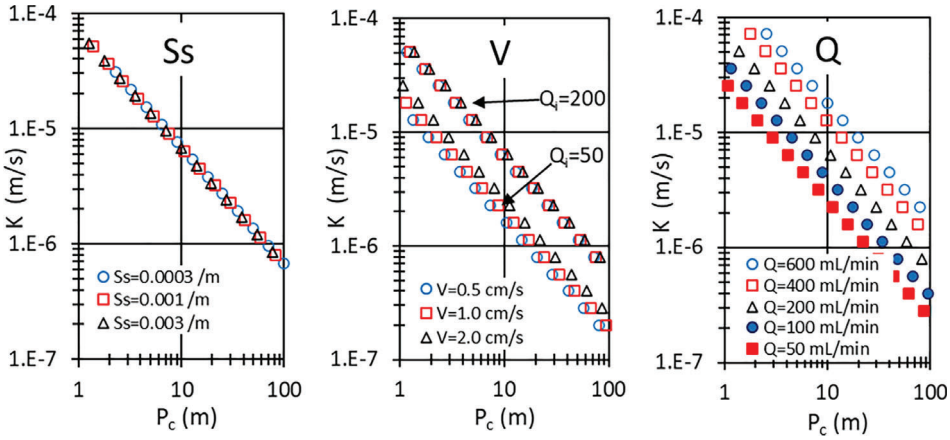


**Figure 4.** $K$ as a function of corrected pressure ($P_c$) for varying specific storage ($S_s$), probe speed ($V$), and injection rate ($Q$). In all three plots, the base case parameter values are $S_s = 0.001$/m, $V = 2$ cm/s, and $Q = 200$ mL/min. In the left plot, $S_s$ is varied between 0.0003 and 0.001/m; in the right plot, $Q$ is varied between 50 and 600 mL/min. In the middle plot, the probe velocity is varied between 0.5 and 2 cm/s at two different flow rates (200 and 50 mL/min).

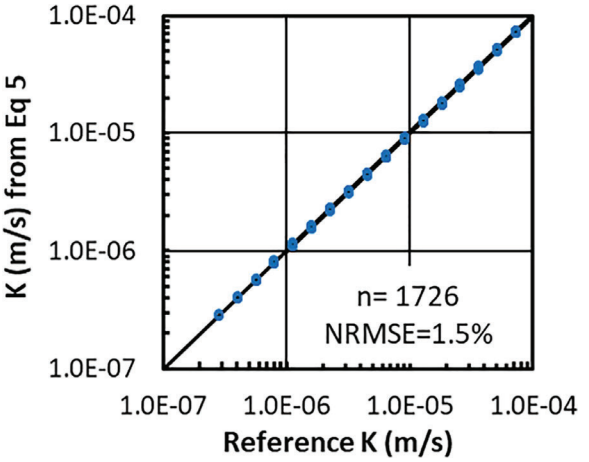


**Figure 5. Comparison of reference $K$ with estimates generated by Equation 5.**

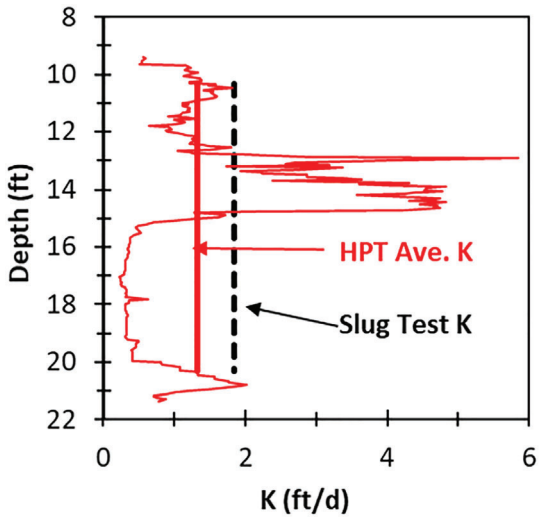


**Figure 6. Comparison of slug test results in monitor well with adjoining HPT profile computed with $E = 1.0$.**

approximately constant for each boring. However, $Q$ was varied between borings ($Q = 100$ to 500 mL/min) to maintain $P_c$ within a measurable range. Data were acquired using the HPT Flow Controller (K6300), Field Instrument (FI6000), and HPT Acquisition Software. $P_c$ was calculated as the total HPT measured pressure minus the sum of hydrostatic pressure ($P_h$) and atmospheric pressure ($P_a$). $P_a$ was measured using the HPT probe with $Q = 0$ at the land surface immediately prior to the start of each boring. $P_h$ was calculated from the measured depth to water in the adjoining monitor well. Profiles of $K$ vs. depth were calculated using Equation 5, generating individual $K$ estimates at 0.05 feet intervals. For comparison with the slug test results, the vertically averaged $K$ is calculated as the arithmetic average of the HPT $K$ values over the saturated screened interval of the adjoining slug test well.

Figure 6 shows an example $K$ profile at the Tulsa site. $K$ was computed from the HPT data assuming $E = 1.0$ (no $K$ reduction in disturbed zone). Most of the flow at this location occurs in a sandy zone extending from about 13 to 15 feet bgs (below ground surface), with much lower $K$ in the overlying and underlying silty zones. Computed $K$ varied from 0.2 to 5.8 feet/d over the screened interval of MW-6 (10.3 to 20.3 feet bgs) with an arithmetic average ($K_{HPT}$) of 1.3 feet/d. In comparison, $K_{slug}$ was 1.85 feet/d, a factor of 1.4 times $K_{HPT}$ in the adjoining HPT boring. The difference in average $K$ between the HPT profile and slug test could be due to compaction and/or mixing of aquifer material in the disturbed zone surrounding the HPT probe, differences in lithology between the well and adjoining HPT boring, as well as the inherent limitations of data and analyses associated with both HPT and the slug test approach.

Results of the slug tests and HPT profiling from 23 locations are summarized in Table S1 in supporting information assuming no permeability loss in the disturbed zone ($E = 1.0$). The ratio of vertically averaged HPT

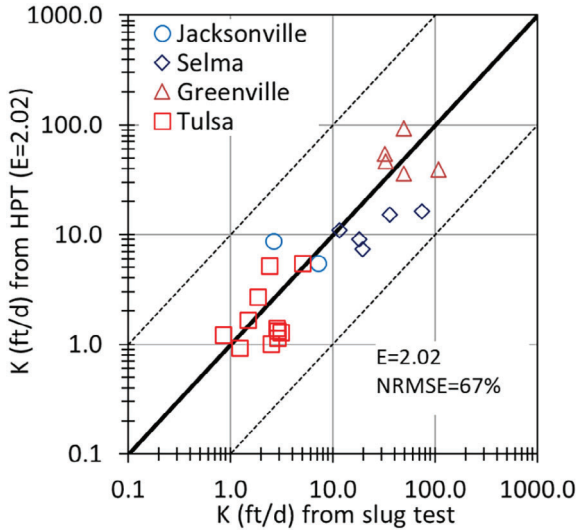


**Figure 7. Comparison of $K$ estimates from slug tests and vertically averaged $K$ from HPT profiling using Equation 5 with $E = 2.02$.**

$K$ to slug test $K$ ($K_{HPT}/K_{slug}$) varied from 0.11 to 1.66 with a mean of 0.49 (std. dev. =0.37, 99% conf. Limit = 0.28 to 0.71) indicating that on average, $K_{HPT}$ is about half of $K_{slug}$ assuming $E = 1.0$. Figure S1 in supporting information is a graph of $K_{HPT}$ vs. $K_{slug}$ for the 23 locations examined. Most points plot below the 45 line, consistent with $K_{HPT} < K_{slug}$. The power law relationship, $K_{HPT} = 0.51\ K_{slug}^{0.87}$, provides the best fit to the data. However, 95% confidence limits for the exponent (0.87) were 0.66 to 1.08 indicating the slope of the relationship was not statistically different from 1.0 at the 95% level. Consequently, the simpler linear relationship, $K_{slug} = E\ K_{HPT}$ where $E = 1/0.49 = 2.02$, is adopted here.

Figure 7 shows a comparison of $K$ measured by slug tests in monitor wells to vertically averaged $K$ estimated using Equation 5 with $E = 2.02$. The average $K$ generated by HPT provided an excellent match to the slug test results. The NRMSE of 67% is very good, given the natural variability in slug test results and that the slug test and HPT profiles were located about 3 feet apart.

### Dependence of $P_c$ on $Q$ and $V$

In both high and low $K$ formations, our ability to reliably measure pressure generated by the HPT tool is the key to accurate $K$ measurement. Temporal variations in atmospheric pressure, shock waves generated by hydraulic hammering, and other factors such as regional groundwater pumping, can all contribute to background noise in HPT pressure measurement, making it difficult to reliably determine $P_c$ within ±0.5 psi (±0.35 m). In high $K$ formations, pressure generated by probing is often less than levels that can be reliably measured (1 psi). In lower $K$ formations, pressures in excess of the maximum measurable pressure (100 psi) can be generated due to fluid displaced by the advancing HPT probe and fluid injection. The allowable operating range for $K$ could potentially be expanded by adjusting the HPT rod speed and the

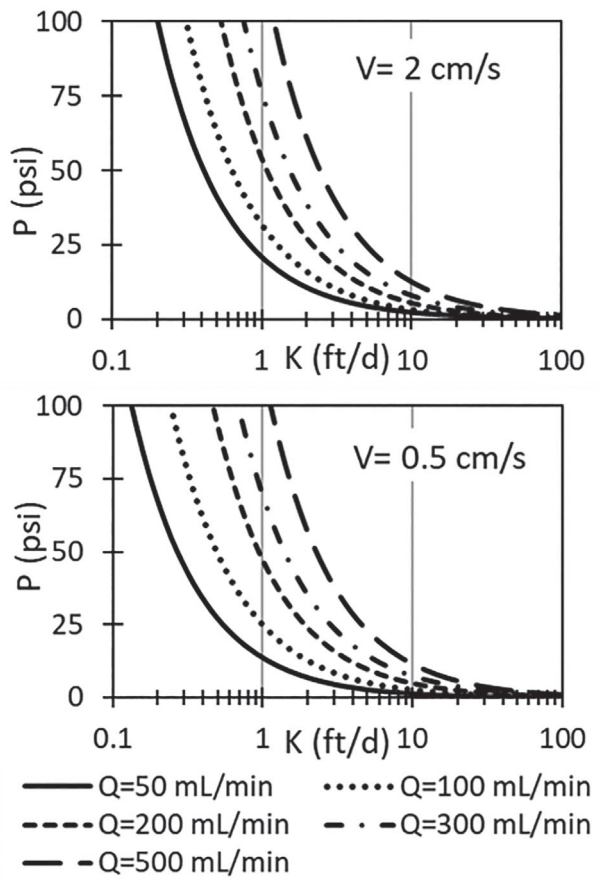


**Figure 8. Total pressure ($P$) generated for varying $Q$ and $K$ at $V = 2$ and 0.5 cm/s.**

injection rate $Q$. Figure 8 shows the pressure generated by the HPT probe at speeds of $V = 2$ and 0.5 cm/s and $Q$ between 50 and 500 mL/min using Equation 5 with $E = 2.02$. At $V = 2$ cm/s and $Q = 500$ mL/min, $P$ exceeds 100 psi for $K < 1.2$ feet/d. However, by reducing $Q$ to 50 mL/min, $K$ values down to 0.21 feet/d could be measured. By reducing the probe speed to 0.5 cm/s, $K$ is further extended to 0.14 feet/d. However, reducing the probe speed would greatly increase probing time, so it is typically not recommended unless $K$ is less than 1 feet/d. A significant advantage of our new $K$ estimation equation over previous approaches is that it explicitly incorporates the impact of probing speed that becomes more important when $Q$ is small in lower $K$ settings.

## Summary

A physically based equation is presented for estimating hydraulic conductivity from $Q$ and $P_c$ measured during HPT profiling. The new $K$ estimation equation (Equation 5) is developed using simulation results spanning a range of formation properties ($K$ and $S_s$) and HPT operating parameters (advance speed and injection rate). Compared to previous work (Dietrich et al. 2008; McCall and Christy 2010), our approach explicitly addresses the effect of HPT probe advance speed, which becomes important for $K$ profiling in less permeable settings

($K < 1$ feet/d) with $Q < 50$ mL/min. When $K$ is lower, the pressure generated by HPT probe advance and water injection can exceed the limit of the pressure sensor, while reducing the injection rate and probe advance speed can reduce the pressure and extend the measurable $K$ range.

The new $K$ estimation equation is evaluated by comparing $K_{HPT}$ to $K_{slug}$ for 23 wells located at four different field sites. Assuming $E = 1.0$, the average ratio of $K_{HPT}/K_{slug}$ was 0.49 (std. dev. $= 0.37$, 99% conf. Limit $= 0.28$ to 0.71), consistent with reduced $K$ in the disturbed zone surrounding the HPT probe. Lower $K$ in the disturbed zone is most likely due to soil compaction and/or shear induced mixing of clayey and sandy layers.

Using the best fit hydraulic efficiency factor ($E$) of 2.02, the HPT results match the slug tests very well. The normalized root mean square error is 67%, indicating the high accuracy of our equation for $K$ estimation under field conditions. Additional research is required to understand the impacts of aquifer characteristics on $E$.

## Acknowledgments

The research presented in this manuscript was supported in part by the Strategic Environmental Research and Development Program (SERDP) under project ER-2529 entitled "Quantifying Mobile-Immobile Mass Transfer using Direct Push Tools."

**Authors' Note:** The author(s) does not have any conflicts of interest.

## Supporting Information

Additional supporting information may be found online in the Supporting Information section at the end of the article. Supporting Information is generally *not* peer reviewed.

**Table S1** in Supporting Information summarizes information on the HPT profiles and slug test wells using in the field evaluation. $K$ values measured by slug test and HPT with $E = 1.0$ are compared in Figure S1. Supporting information is generally not peer reviewed.

## References

American Society of Testing and Materials (ASTM). 2016. *D8037 Standard Practice for Direct Push Hydraulic Logging for Profiling Variations of Permeability in Soils*. West Conshohocken, Pennsylvania: ASTM International.

Beckie, R., and C.F. Harvey. 2002. What does a slug test measure: An investigation of instrument response and the effects of heterogeneity. *Water Resources Research* 38, no. 12: 26–21.

Borden, R.C., K.Y. Cha, R. Falta, and G. Liu. 2020, Quantifying mobile-immobile mass transfer using direct push tools, ER-2529, Final Technical Report, Strategic Environmental Research and Development Program, Arlington, Virginia.

Bouwer, H., and R.C. Rice. 1976. A slug test for determining hydraulic conductivity of unconfined aquifers with completely or partially penetrating wells. *Water Resources Research* 12, no. 3: 423–428.

Brown, D.L., T.N. Narasimhan, and Z. Demir. 1995. An evaluation of the Bouwer and Rice method of slug test analysis. *Water Resources Research* 31, no. 5: 1239–1246.

Burns, S.E., and P.W. Mayne. 1998. Monotonic and dilatory pore-pressure decay during piezocone tests in clay. *Canadian Geotechnical Journal* 35, no. 6: 1063–1073.

Butler, J.J. Jr. 2019. *The Design, Performance, and Analysis of Slug Tests*, 2nd ed. Florida: CRC Press 280p.

Chapuis, R.P., and M. Aubertin. 2003. On the use of the Kozeny Carman equation to predict the hydraulic conductivity of soils. *Canadian Geotechnical Journal* 40, no. 3: 616–628.

Cho, H.J., R.J. Fiacco Jr., M. Horesh, J. Picard, S. Pitkin, E. Madera, and E. Rasmussen. 2004. Evaluation of the Waterloo profiler as a dynamic site investigation tool. In *Proceedings of the Fourth International Conference on Remediation of Chlorinated and Recalcitrant Compounds*, ed. A.R. Gavaskar, and A.S.C. Chen. Columbus, Ohio: Battelle Press. Paper 1B-07.

Dietrich, P., and C. Leven. 2009. Direct push-technologies. In *Groundwater Geophysics*, ed. R. Kirsch. Berlin, Heidelberg, Germany: Springer.

Dietrich, P., J.J. Butler Jr., and K. Faiss. 2008. A rapid method for hydraulic profiling in unconsolidated formations. *Groundwater* 46, no. 2: 323–328. https://doi.org/10.1111/j.1745-6584.2007.00377.x

Freeze, J.A. & Cherry, R.A. 1979. Groundwater. Englewood Cliffs, New Jersey: Prentice-Hall.

Geoprobe. 2015. Geoprobe® hydraulic profiling tool (HPT) system standard operating procedure. Technical Bulletin No. MK3137. Kejr Inc./Geoprobe Systems, Salina, KS. January.

Lessoff, S.C., U. Schneidewind, C. Leven, P. Blum, P. Dietrich, and G. Dagan. 2010. Spatial characterization of the hydraulic conductivity using direct-push injection logging. *Water Resources Research* 46: W12502. https://doi.org/10.1029/2009WR008949

Liu, G., J.J. Butler Jr., E.C. Reboulet, and S. Knobbe. 2012. Hydraulic conductivity profiling with direct push methods. *Grundwasser* 17, no. 1: 19–29. https://doi.org/10.1007/s00767-011-0182-9

Liu, G., J.J. Butler Jr., G.C. Bohling, E. Reboulet, S. Knobbe, and D.W. Hyndman. 2009. A new method for high-resolution characterization of hydraulic conductivity. *Water Resources Research* 45: W08202. https://doi.org/10.1029/2009WR008319

Liu, G., R.C. Borden, and J.J. Butler Jr. 2019. Simulation assessment of direct push injection logging for high-resolution aquifer characterization. *Groundwater* 57, no. 4: 562–574.

Maliva, R.G. 2016. Direct-push technology. In *Aquifer Characterization Techniques*. Springer, Cham, Switzerland: Springer Hydrogeology.

McCall, W., T.M. Christy, and M.K. Evald. 2017. Applying the HPT-GWS for hydrostratigraphy, water quality and aquifer recharge investigations. *Groundwater Monitoring & Remediation* 37, no. 1: 78–91. Winter.

McCall, W., and T.M. Christy. 2010. Development of a hydraulic conductivity estimate for the Hydraulic Profiling Tool (HPT), The 2010 North American Environmental Field Conference & Exposition: Conference Program with Abstracts: Session VII.

Schulmeister, M.K., J.J. Butler, J.M. Healey, L. Zheng, D.A. Wysocki, and G.W. McCall. 2003. Direct-push electrical conductivity logging for high-resolution hydrostratigraphic characterization. *Groundwater Monitoring & Remediation* 23, no. 3: 52–62.

Zlotnik, V.A., D. Goss, and G.M. Duffield. 2010. General steady-state shape factor for a partially penetrating well. *Groundwater* 48, no. 1: 111–116.